BUOYANCY OF THE "Y2K" PERSISTENT TRAIN AND THE TRAJECTORY OF THE 04:00:29 UT LEONID FIREBALL

PETER JENNISKENS
SETI Institute, NASA ARC, Mail Stop 239-4, Moffett Field, California 94035
E-mail: pjenniskens@mail.arc.nasa.gov

and

RICK L. RAIRDEN
Lockheed Martin Space Sciences LaboratoryDept L9-42, Bldg 255, 3251 Hanover Street, Palo Alto, California 94304
E-mail: rairden@spasci.com

(Received 23 June 2000; Accepted 29 July 2000)

Abstract. The atmospheric trajectory is calculated of a particularly well studied fireball and train during the 1999 Leonid Multi-Instrument Aircraft Campaign. Less than a minute after the meteor's first appearance, the train curves into a "2"-shape, which persisted until at least 13 minutes after the fireball. We conclude that the shape results because of horizontal winds from gravity waves with a scale height of 8.3 km at 79–91 km altitude, as well as a westerly wind gradient with altitude. In addition, there is downward drift that affects the formation of loops in the train early on.

Keywords: Fireball, leonids 1999, lower thermosphere, mesosphere, meteor, persistent train, winds

1. Introduction

A bright fireball of absolute magnitude about –13 appeared over the isle of Corsica at 04:00:29 UT in the night of November 18, 1999. The fireball registered on three slit-less spectrographs onboard the Leonid Multi-Instrument Aircraft Campaign, probing various wavelength ranges in the near-UV, visual and optical near-IR. The fireball provided the first spectrum of a meteor's afterglow, which made it possible to study the cooling rate of the emitting gas in the first seconds after the meteor (Borovicka and Jenniskens, 2000). Once the afterglow had subsided, a luminous glow persisted for more than 13 minutes. Such persistent trains have eluded a better understanding for over a century (Lockeyer, 1869).

The train provided the first mid-IR spectroscopy (Russell *et al.*, 2000), and was observed by other techniques as well.

All observed physical conditions are a function of altitude. The two participating aircraft in Leonid MAC, the "Advanced Ranging and Instrumentation Aircraft" [ARIA] and the "Flying Infrared Signatures Technology Aircraft" [FISTA], offered two perspectives that made triangulation possible (Jenniskens and Butow, 1999). In this paper, we calculate the trajectory of the fireball from the available optical records, providing height and range information for each part of the train. The meteor was only observed from ARIA but the persistent train was observed from both aircraft. The train record from FISTA is of high spatial resolution, which enables us to trace the train back to its point of origin. This is made easy because the train has 'billowing' structures that stand out for the entire period of observation.

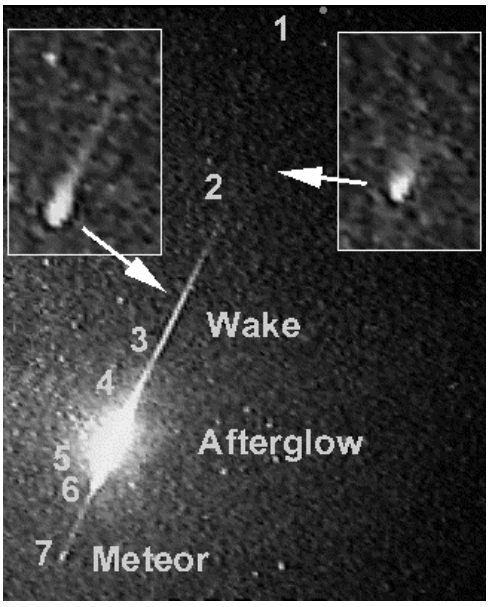

Figure 1. The 04:00:29 UT meteor and its afterglow. Inserts show the onset of persistent emission.

Horizontal winds and vertical drifts are responsible for the observed shape changes of the persistent train over time. Strong horizontal winds are caused by gravity waves in the ambient atmosphere. Vertical drifts may result from the buoyancy of the heated air in the path of the meteor.

Especially the latter aspect is of interest in understanding the physical conditions in the meteor path. We have examined the observations for evidence of such vertical motions

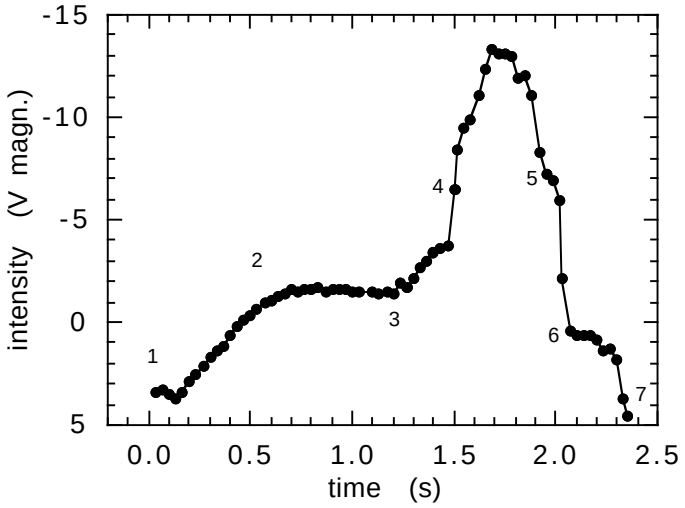

Figure 2 The visual light-curve magnitude of the meteor (normalized at 100 km distance) versus time. Markers as shown in Figure 1.

2. The observations

2.1. THE FIREBALL

The fireball was observed by a wide angle Mullard XX1332-intensified Hi-8 camera (Jenniskens, 1999) onboard ARIA (Figure 1). The video record was digitized with 640 x 480 resolution elements. Figure 1 is taken from a single frame shortly after the bright flare. The full frame is shown in Borovicka and Jenniskens (2000). Note that a small fragment of the meteor survives to the low altitude marker [7]. The field of view of the image is about 20 x 25 degrees. The meteor entered the frame at the top of the field as a faint point source (marker [1]). It soon spreads into the characteristic V-shaped structure first recognized by Spurny *et al.* (2000a). Shortly after, it turns into a droplet shape and at the same

time starts to create a wake that persists for two seconds (Figure 1; [2]). At lower altitude, it rapidly brightens [3], followed by a sudden increase in brightness [4]. The persistent train originates from the part of the meteor's trajectory between [4] and [5]. The meteor then fades into a point source [6], which persists for a short period until time marker [7].

The light-curve shown in Figure 2 was reconstructed from the video record, after calibration of the blooming pattern in the intensified camera, and with help of a reflected image in an adjacent ARIA camera. The absolute peak-brightness of the meteor is about –13 magn., which would correspond to a mass of about 1 kg for this meteoroid (Spurny *et al.*, 2000b). At the peak of the light curve, a series of abrupt brightness changes occurred within a single frame that were only recognized clearly in the spatial pattern of the afterglow (Borovicka & Jenniskens, 2000).

2.2. THE AFTERGLOW

A bright afterglow is seen at the position of the intense flare in Figure 1, which persisted for about 5 seconds. This emission is due to low-excitation neutral atom emission lines that are discussed in Borovicka and Jenniskens (2000).

2.3. THE PERSISTENT TRAIN

Once the afterglow has faded, persistent emission remains that was nearly constant in intensity along the path of the meteor (Figure 3). This persistent train is initially a straight line. It stretches only from about point 4 to 5, where the meteor is brighter than the typical train-forming threshold of about –4 magnitude (Jenniskens *et al.*, 1998). Subsequently, "S"-shaped structures form at three different positions in the train, making a corkscrew pattern with large separation between the tightly wounded curls. First, the lower half of the train quickly fades in intensity, wrinkles, and forms a curl (Figure 3 at time 0:38; see also Figure 4). In the middle of the train, a second curl formed that gradually brightens and lengthens in the horizontal direction, whereby its upper part appears to move downward (Figure 3). Finally, at the top of the train another curl forms more gradually, by what initially appears to be a settling motion to establish its “foot”. The lower part of this curl subsequently stretches out and retains a relatively high intensity, while the upper part is soon undetectable.

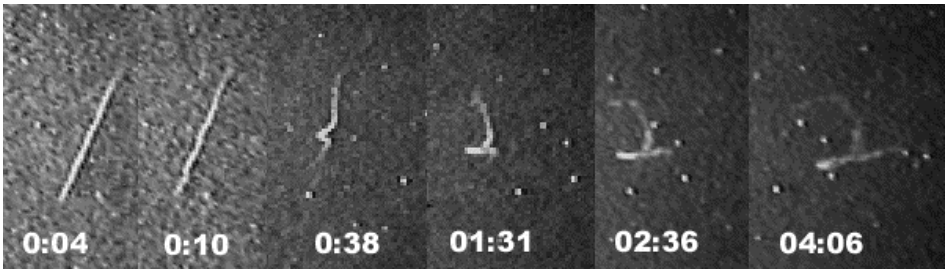

Figure 3 The persistent train as seen from ARIA at different times following the meteor (in minutes and seconds).

After about 1.5 minutes from the time of the meteor (1:31 in Figure 3) the basic shape of a "2" is formed as a composite of the middle curl and the foot of the top curl. Because of its striking shape and occurrence, this particular nature's-own end-of-the-millennium fireworks was soon named the "Y2K train". The "2"-shaped feature, including its many 'billowing' features, does not significantly change over the next 12 minutes (Figure 5). Aircraft motion causes a gradual, but not substantial, drift in azimuth as seen by the projection of the train against the star background (Figure 3). The train was observed until 04:13:29 UT, when it drifted outside the field of view of the ARIA camera.

Figure 4. First view from FISTA 50 seconds after fireball (camera: FH50R). Notice the corkscrew pattern.

In response to the unusual sighting, the FISTA aircraft quickly changed its direction in order to bring this train into view of its onboard cameras and spectrometers. The earliest record is taken with the upward looking camera FH50R, only 48 seconds after the meteor appeared (Figure 4). The corkscrew pattern is clearly visible with most of the light intensity now being in the middle and upper parts of the train.

A particularly nice image was recorded with an UV sensitive Xybion intensified CCD camera (Figure 5). With a field of view of only 8.6 x 11.5 degrees that offered the best spatial resolution, while having most of the train in the field of view for the entire event. It was filmed from 3m38s until 8m20s after the meteor's first appearance. The train stays together, with no noticeable expansion or diffusion over the course of the experiment but its internal structures become gradually diffuse. Yet, the 'billowing' features remain visible over the entire period.

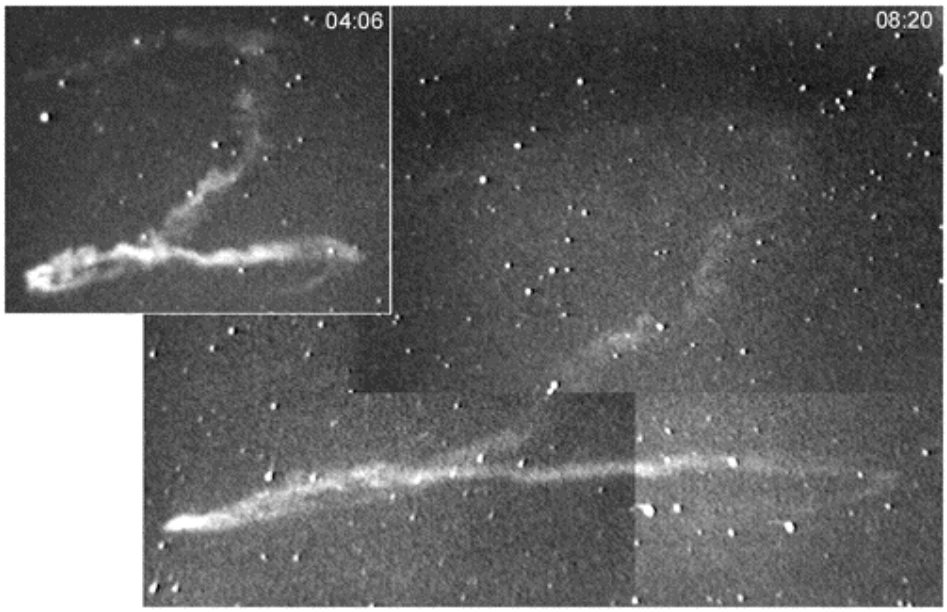

Figure 5. Persistent train as seen from FISTA at times 04:06 and 08:20 (Xybion camera).

3. TRIANGULATION OF THE TRAIN AT 04:04:35 UT

We identified 29 features in the train that can be used to trace changes in the horizontal winds. First, we calculated the position of each feature by triangulation of these individual features. The result is shown in Figure 6 wherein the position of each feature is indicated by a black dot. The numerical results are summarized in Table I, where each feature is numbered from the top down. The upper part of the "2" is situated at an altitude of 91 km, while the curl making its "foot" is at around 84 km.

The lowest visible part of the train (at time 04:06) is at about 79 km altitude.

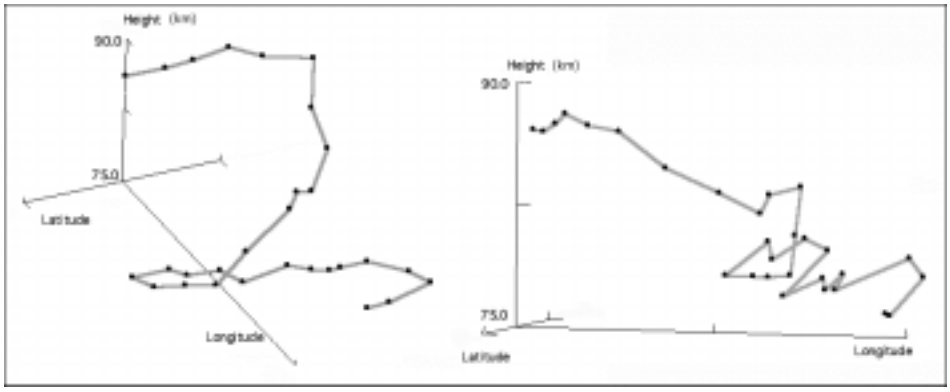

Figure 6. The 3-dimensional structure of the train at 04:04:35 UT, at time 04:06 after the meteor from two perspectives. The positions of train features are indicated.

TABLE I

#	H (km)	R (ARIA) (km)	R (FISTA) (km)	#	H (km)	R (ARIA) (km)	R (FISTA) (km)
1	91.6 ± 3	308 ± 6	191 ± 4	16	82.6	320	203
2	90.9	304	189	17	84.2	320	205
3	91.0	303	188	18	83.2	319	204
4	91.0	300	187	19	83.8	318	205
5	90.2	302	191	20	83.2	318	205
6	89.7	296	186	21	80.3	309	197
7	88.4	300	189	22	81.3	310	199
8	86.7	302	191	23	80.5	309	198
9	85.5	312	195	24	81.4	309	199
10	86.3	309	197	25	80.5	306	196
11	86.6	312	201	26	81.7	308	200
12	85.9	316	202	27	80.5	307	200
13	82.1	318	203	28	79.2	308	199
14	82.1	318	203	29	79.3	310	200
15	82.4	331	216				

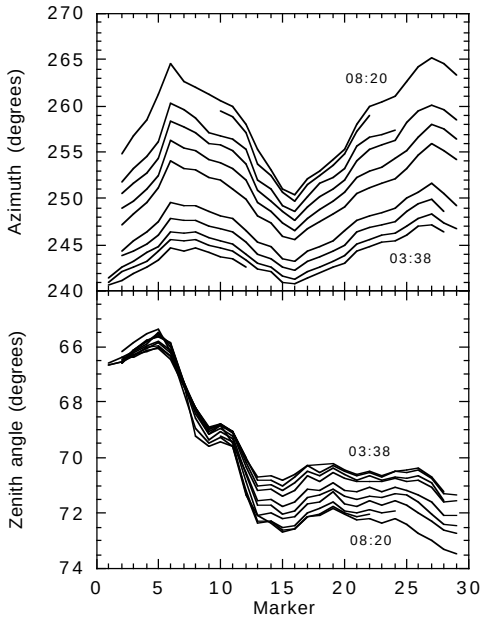

Figure 7. Train drift in azimuth (top) and zenith distance angle (bottom) as seen from the FISTA aircraft. Markers are positions defined in Figure 6.

3.1. TRAIN DRIFT AFTER 01:30

The observed train drift after time 01:30 can be traced back to the time of the fireball, thus providing a record of the position of the meteor as seen from FISTA. For that purpose, we use the images in Figure 5 that were taken between times 3:38 and 8:20. Figure 7 shows the azimuth and zenith distance angle for the 29 positions along the train, as defined in Figure 6, at ten different times during this interval. In this paper azimuth is expressed as an angle from South over West. The particular choice of ten times is dictated by the video record obtained by a hand-pointed camera that only occasionally provided images that were suitable for analysis.

The change in azimuth is unremarkable (closed points in Figure 8). There is a linear component that is caused by the near-linear aircraft motion (Figure 9) and an altitude-dependent variation that is a signature of gravity waves. The change in zenith distance also varies with altitude (open points in Figure 8), but is not easily understood. The lower parts of

the train gradually decline in elevation, which is mostly an effect of the aircraft moving away from the train. The expected effect is an increase in zenith distance by about 0.012 deg/s. The upper part, above marker point 14 (above the foot of the "2") stays at nearly constant elevation. This implies that the train drifts either towards FISTA (in west/southwestward direction) at a rate of about 70 m/s, or this part of the train moves upward at a rate of about 25 m/s, relative to the train below marker 14. A relative 75 m/s west/northwestward drift is implied by the shape of the train in Figure 6, suggesting that most of the effect is in fact due to a horizontal wind gradient with altitude.

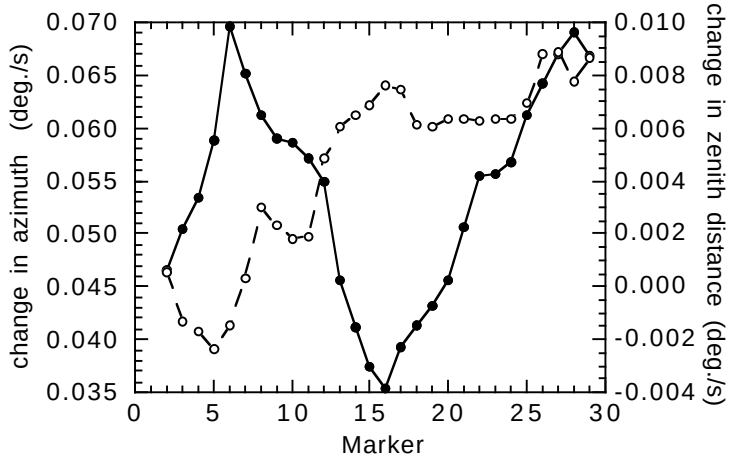

Figure 8. Mean rate of change in azimuth and zenith distance between times 03:38 and 08:20.

3.2. TRIANGULATION OF THE METEOR

By extrapolating the train motion backward in time, we can reconstruct the position of the meteor as seen from FISTA and calculate the trajectory by comparison with the meteor record from ARIA (Figure 1). We use the fact that the FISTA aircraft motion was almost linear during the period of interest (03:38–08:20), as shown in Figure 9. Figure 10 shows the resulting position of each marker point, in azimuth and zenith distance as seen from FISTA. We show the results for both linear and a parabolic extrapolations of the observed trend of position versus time for each feature in the train.

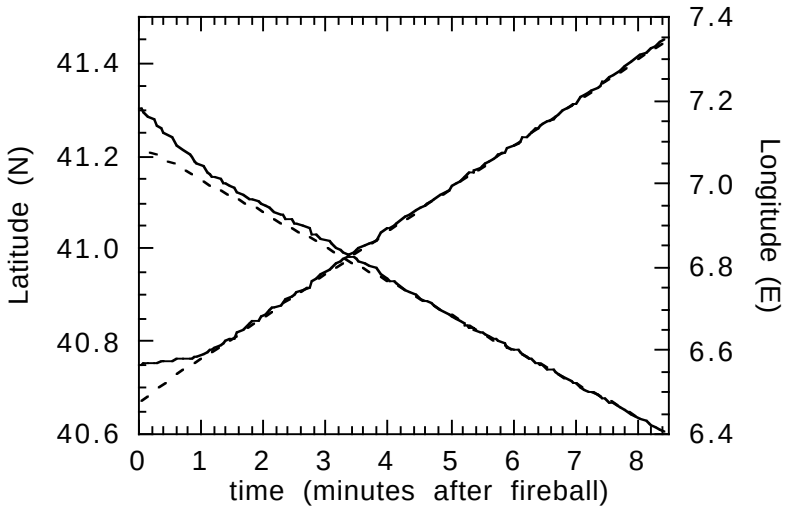

Figure 9 Change of the geographic position of the FISTA aircraft during the time of observation of the "Y2K" persistent train.

The convergence angle between the two planes that are defined by the position of the aircraft and the projection of the meteor against the sky is only 12º. In order to arrive at the correct trajectory, we made the assumptions that the radiant of the meteor is that of the Leonid shower (RA = 153.1 º, DEC = 22.7 º J2000) and the average meteor speed is that of the Leonids: 71.5 km/s (Jenniskens *et al.*, 1998). The radiant direction was towards Azimuth = 309 º (SE) and Zenith Distance = 31º. These are strong constraints that leave little room for a wrong fit. The change in azimuth and zenith distance for different positions of the meteor trajectory as seen from FISTA is shown in Figure 10. The direction of the Leonid radiant determines the slope of the dashed line. It is clear that the “foot” of the "2"-shaped train feature at about 81 km altitude stands out as having significant motion in azimuth other than caused by the aircraft’s motion. The motion in azimuth causes the initial stretching of the middle curl (Figure 3).

For any reasonable fit of the meteor’s azimuth direction, we can only find a computational solution matching the altitudes of position marker points if the zenith distance of the meteor is about two degrees higher than was back-calculated from the extrapolation of the marker points (lower part Figure 10). The speed of the meteor is also an important

additional constraint, because it defines the length of the observed trajectory and thus the position of the meteor's path in distance from the aircraft. No reasonable solution is obtained for a fit differing more than ±0.4 degree in zenith distance from that shown as a dashed line in Figure 10. If the zenith distance is as low as implied by the data in Figure 10 the computed solution for the speed of the meteor will be too high and hence the trajectory too far from both aircraft.

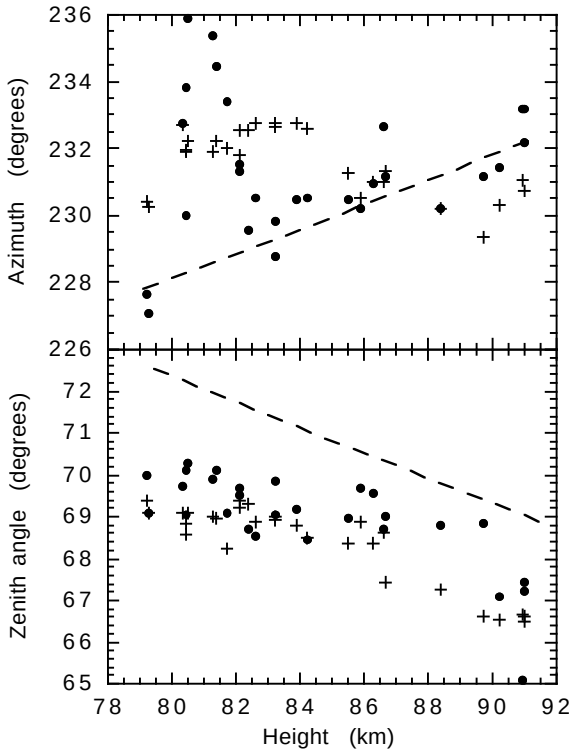

Figure 10. Azimuth and zenith distance angle of the meteor itself as seen from FISTA. The position of the meteor is derived from assumed linear (+) or parabolic (•) extrapolation of train drift. Dashed lines show the trajectory that provides the best triangulation results with ARIA.

The reason for this discrepancy remains unknown. However, the best fitted meteor trajectory (dashed line) is in good agreement with other Leonid fireball trajectories, with key features at similar altitudes. The meteor discussed here was first detected at about 195 km altitude and ended the so-called ‘diffuse phase’ (Spurny *et al.*, 2000a) at about 136

km altitude. This compares to 195 km and 134–131 km for a –12.5 magnitude Leonid fireball DMS98023 studied by Spurny *et al.* (2000b). The rapid increase in intensity associated with the ablation of silicates (Borovicka *et al.*, 1999) occurred at about 100 km altitude. The bright burst in the train discussed here started at 89-km altitude and lasted until 74-km altitude. The decay in brightness was complete only at 71 km altitude. This compares to a photographic end height of the train at 73.2 km for DMS98023 (Spurny *et al.*, 2000b). A small but structurally coherent fragment of the meteor continued to an unusually low altitude of 55 km.

4. Discussion

We submit that vertical motions are important in the early dynamic evolution of the persistent train of the meteor described here. The formation of "S"-shaped features, and significant stretching of the lower part of those structures shortly after train formation appears to be the result of settling of air in the path of the meteor. Judging from the differences in the initially-formed shape and those that formed later, this phenomenon is not a mere reflection of periodic winds in the ambient air. The settling motion is surprising because heated air will flow upward. On the other hand, the heated gas is expected to expand rapidly after the meteor until pressure equilibrium is established, probably in a manner of seconds. Subsequent cooling of the buoyant air can lead to flow downward until pressure equilibrium is established. The observed ‘billowing’ features are remarkably constant in time. They must have formed early on during formation, possibly as a result of the intensity variations across the meteor's path that are so conspicuous in the afterglow images.

At later times, ambient winds dominate the change in shape and train expansion. When the 3-dimensional solution of the train geometry is viewed at an angle about 90 degrees from the lines of sight from ARIA and FISTA (Figure 6), a more or less linear appearance of the train results. We considered that this might be an artifact of triangulation because both trains are relatively distant from the observing aircraft. By imposing a periodic wind variation on the solution, we attempted to recreate the "2" shape in a model. The best solution reflects a periodic wind variations between 79 and 91 km with an amplitude of 57 ± 8 m/s and a vertical scale length of 8.3 ± 0.5 km (Figure 11). The shape of the "2" is only well reproduced if a vertical wind gradient is included.

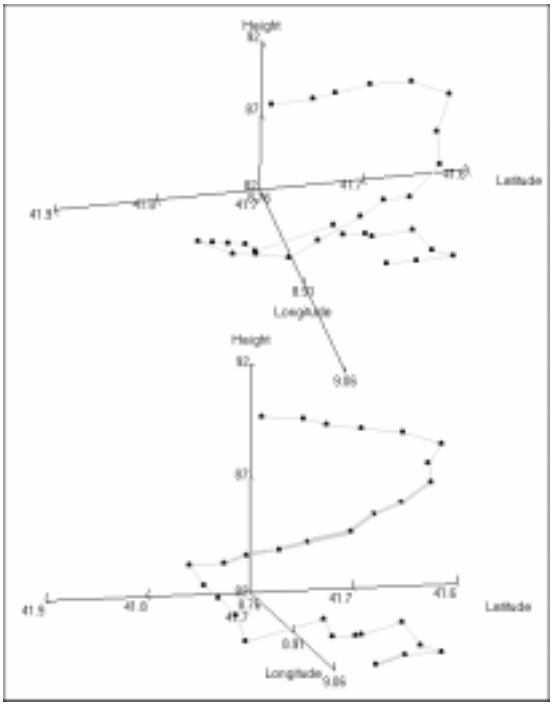

Figure 11. Model of the Y2K train at 04:04:35 UT by imposing a periodic wind variation with altitude but without a wind gradient.

Radar wind measurements in middle-Europe (Singer *et al.*, 2000) showed tidal wind oscillations with an amplitude of about 40 m/s and a scale height of about 8.5 km between 85 and 105 km altitude. At 04 UT, the zonal winds were changing in direction from east to west, more quickly at higher altitude. These observations are consistent with the observed east-west gradient in Figure 6.

Acknowledgements

We are grateful for the constructive reviews by Jack Drummond and Frans Rietmeijer to improve the presentation of this paper. Klaas Jobse operated the Mullard XX1332-intensified Hi-8 camera onboard ARIA. Mike Koop operated the FH50R camera on FISTA. The 1999 Leonid MAC was sponsored by the NASA Exobiology, Planetary Astronomy,

and Suborbital MITM programs, by the Advanced Missions and Technologies for Astrobiology Program, and by NASA Ames Research Center. ARIA flight time was supported by the USAF/XOR. *Editorial handling:* Frans Rietmeijer.

References

Borovicka, J. and Jenniskens, P.: 2000, *Earth, Moon and Planets* **82–83**, 399–428.
Borovicka, J., Stork, R., and Bocek, J., 1999: *Meteoritics Planet. Sci.* **34**, 987–994.
Jenniskens, P.: 1999, *Meteoritics Planet. Sci.* **34**, 959–968.
Jenniskens, P. and Butow, S.J.: 1999, *Meteoritics Planet. Sci.* **34**, 933–943.
Jenniskens, P., de Lignie, M., Betlem, H., Borovicka, J., Laux, C.O., Packan, D., and Kruger, C.H.: 1998, *Earth, Moon and Planets* **80**, 311–341.
Lockeyer, N.: 1869, *Nature* **1**, 58.
Russell, R., Rossano, G., Catelain, M.A., Lynch, D., Tessensohn, T., Abendroth, E., and Jenniskens, P.: 2000, *Earth, Moon and Planets* **82–83**, 439–456.
Singer, W., Hoffmann, P., Mitchell, N.H., Jacobi, Ch.: 2000, Earth, Moon and Planets **82–83**, 565–575.
Spurny, P., Betlem, H., Jobse, K., Koten, P., and Van 't Leven, J.: 2000a, *Meteoritics Planet. Sci.* **35(5)**, in press.
Spurny, P., Betlem, H., van 't Leven, J., and Jenniskens, P.: 2000b, *Meteoritics Planet. Sci.* **35**, 243–249.